Resonance Energy Transfer as a Monitor of Membrane Protein Domain Segregation: Application to the Aggregation of Bacteriorhodopsin Reconstituted into Phospholipid Vesicles†

C. A. Hasselbacher, Terry L. Street, and T. G. Dewey*

ABSTRACT: Resonance energy transfer has been used to monitor the aggregation of proteins in membranes. Bacteriorhodopsin reconstituted into phospholipid vesicles was used as a model system to investigate the sensitivity of energy transfer to protein domain or patch formation. The state of aggregation of the bacteriorhodopsin was controlled by adjusting the temperature. It is well established that bacteriorhodopsin will aggregate at temperatures well below the lipid phase transition. These aggregates melt out to form monomers at temperatures slightly below the lipid phase transition. Energy transfer was measured from rhodamine or indocarbocyanine lipid donors to the retinal of the protein. Steady-state measurements of the efficiency of energy transfer showed a significant decrease at low temperatures. This is due to the inefficient transfer to acceptors buried in the interior of the aggregate. A series of approximate expressions were derived and are used to analyze the data quantitatively. The radius of the aggregated patch can be determined from this analysis. Our results indicate that the average patch radius is independent of bacteriorhodopsin surface density at densities above a critical level. The patch size decreased with temperature and was dependent on the type of lipids in the vesicle. Our results show that energy transfer can be used to observe the segregation of membrane proteins into domains. Quantitative analyses are possible when the segregated domains have radii ranging from 30 to 300 Å.

Resonance energy transfer is a well established technique for measuring distances in biological systems. Most applications of this technique determine a distance between a single donor and a single acceptor [for a review, see Stryer (1978)]. Recent studies on membrane systems present a situation where energy transfer from multiple donors to multiple acceptors must be considered (Hammes, 1981). This more complicated situation has been the subject of several theoretical analyses (Wolber & Hudson, 1979; Dewey & Hammes, 1980; Snyder & Freire, 1982). Most experimental applications to membrane biochemistry use energy transfer to determine either the surface density of the acceptor (Fung & Stryer, 1978) or the distance of closest approach of a donor to an acceptor (Fleming et al., 1979; Rehorek et al., 1983). More complicated situations such as energy transfer between separated spheres have also been considered (Baird et al., 1979).

In the present work resonance energy transfer is used to monitor the aggregation of a membrane protein, bacteriorhodopsin, into a patch or segregated domain. Lipid fluorescence donors will transfer energy much less efficiently to acceptors located in the interior of the patch compared with acceptors located on the boundary of the patch. Patch formation results in a decrease in energy transfer. A theoretical analysis of two-dimensional fluorescence energy transfer from donors in a plane to acceptors in a circular patch is presented. A series of approximate expressions are derived from a general theoretical technique presented previously (Dewey & Hammes, 1980). This theory is used to analyze the experimental data on bacteriorhodopsin aggregation presented in this paper. The efficiency of energy transfer from a fluorescent lipid donor to the acceptor, the retinal of bacteriorhodopsin, has been measured for both bacteriorhodopsin monomers and aggregates. From the theoretical analysis the radius of the bacteriorhodopsin patch is determined.

Bacteriorhodopsin reconstituted into phospholipid vesicles provides a convenient model system to determine the utility of this resonance energy transfer technique. It has been well established by a variety of techniques that bacteriorhodopsin will form aggregates at temperatures well below the lipid phase transition (Heyn et al., 1981a,b). When the temperature is raised to within a few degrees of the lipid transition temperature, the aggregates melt out into monomers. Thus, the state of aggregation of this protein can be controlled by adjusting the temperature. In this work energy transfer is observed both above and below the aggregation temperature of bacteriorhodopsin. The decrease in the efficiency of energy transfer at low temperature is analyzed in terms of the aggregate patch size. Patch radii are determined for two different donors in two different types of phospholipid vesicles. Similar results were obtained under this variety of conditions. These results suggest that resonance energy transfer can be used to quantitate the patching of membrane-bound proteins.

Materials and Methods

Chemicals. Dimyristoylphosphatidylcholine (DMPC),[1] dipalmitoylphosphatidylcholine, and *n*-octyl β-D-glucopyranoside (octyl glucoside) were obtained from Sigma and used without further purification. The fluorescent-labeled lipids, octadecyl rhodamine B chloride and 1,1′-dioctadecyl-3,3,3′,3′-tetramethylindocarbocyanine perchlorate (C_{18}DiI), were purchased from Molecular Probes. All other chemicals were reagent grade, and all solutions were made in distilled deionized water.

Purple Membrane and Reconstituted Vesicles. Halobacterium halobium S-9 was grown on defined media (Lanyi & MacDonald, 1979). Purple membrane fragments were purified

† From the Department of Chemistry, University of Denver, Denver, Colorado 80208. *Received April 30, 1984.* This research was supported in part by Research Corporation Grant 9571 and NSF Grant PCM-8315263. C.A.H. is a Boettcher Foundation Fellow.

[1] Abbreviations: DMPC, dimyristoylphosphatidylcholine; DPPC, dipalmitoylphosphatidylcholine; C_{18}DiI, 1,1′-dioctadecyl-3,3,3′,3′-tetramethylindocarbocyanine perchlorate; OR, octadecylrhodamine B chloride; BR, bacteriorhodopsin; CD, circular dichroism; Tricine, *N*-[tris(hydroxymethyl)methyl]glycine; EDTA, ethylenediaminetetraacetic acid; ATPase, adenosinetriphosphatase.

0006-2960/84/0423-6445$01.50/0

by using a sucrose step gradient (Becher & Cassim, 1975). For vesicle preparation, the desired amount of the fluorescent-labeled lipids was dissolved in chloroform (1 mg/mL) and put into a test tube, and the solvent was evaporated under nitrogen. DMPC or DPPC and Tricine buffer (50 mM Tricine, 0.15 M KCl, pH 8.0) were added, and vesicles were formed by sonication at a temperature above the phase transition of the lipid. Lipid concentrations were 20 mg/mL. Purple membrane was reconstituted into sonicated vesicles by incubation on ice in the dark in the presence of 1.15% octyl glucoside for 1 h. The octyl glucoside concentration was reduced in the samples by dilution over 100-fold in Tricine buffer with 5 mM EDTA. Bleached bacteriorhodopsin was prepared by illumination of a purple membrane sample in the presence of sodium borohydride using a Shoeffel 150-W xenon arc lamp filtered by a Corning CS 1-75 UV–IR filter.

As a check for the homogeneity of the vesicle preparations, the reconstituted vesicles containing OR were centrifuged on a sucrose gradient (5–40%). A single sharp band was observed in the 20% layer. Over 90% of both the BR tryptophan and OR fluorescence was contained in this band. This indicates a fairly homogeneous population of vesicles with respect to size and protein content.

The surface density, σ, of BR was calculated by assuming a surface area of 875 Å^2 for a BR molecule (Henderson & Unwin, 1975) and a surface area of 60 Å^2 per phospholipid. By use of these values, $\sigma = [875\ \text{Å}^2 + (60\ \text{Å}^2)C_L/(2C_{BR})]^{-1}$ where C_L and C_{BR} are the molar concentrations in the reconstitution mixtures of lipid and bacteriorhodopsin, respectively. An extinction coefficient of 54 600 M^{-1} cm^{-1} was used to determine C_{BR} from the absorbance at 560 nm. This is equivalent to the literature value of 56 000 M^{-1} cm^{-1} at 568 nm (Ebrey et al., 1977). A molecular weight of 26 000 was assumed for bacteriorhodopsin. No attempt was made to correct the surface density for changes due to the temperature dependence of surface density of the lipid. Final molar lipid to dye ratios were approximately 200:1; final molar lipid to BR ratios varied from approximately 200:1 to 1000:1.

Spectroscopic Measurements. The amount of quenching of the fluorescent lipid was determined by comparing the ratio of fluorescence of vesicles containing incorporated BR to the fluorescence of vesicles containing donor only (for the fixed temperature studies, see Figures 3 and 4) or donor and bleached BR (for the fluorescent intensity vs. temperature scans, see Figure 2). Fluorescent intensity vs. temperature scans obtained with vesicles containing donor only as a blank and vesicles containing donor and bleached BR as a blank are identical except for slight differences in the slope and width of the curve in the temperature region within ±3 °C above and below the lipid phase transition temperature. The largest variation between the fluorescence of the two samples in this region is approximately 8%. The fluorescence of each sample was recorded at an excitation wavelength of 530 nm for rhodamine and 540 nm for C_{18}DiI, and emission wavelengths were 580 and 568 nm, respectively.

Final lipid concentrations were approximately 0.05 mg/mL. At this concentration light scattering and inner filter effects are insignificant. This was demonstrated by making measurements with different excitation slit widths (1–5 nm) and using cells with different path lengths (2–10 mm). Efficiencies found under these different conditions were identical. A sample of vesicles at this concentration with incorporated BR but no fluorescent donor gave no fluorescent signal, further demonstrating an absence of light scattering or contaminating fluorescence artifacts.

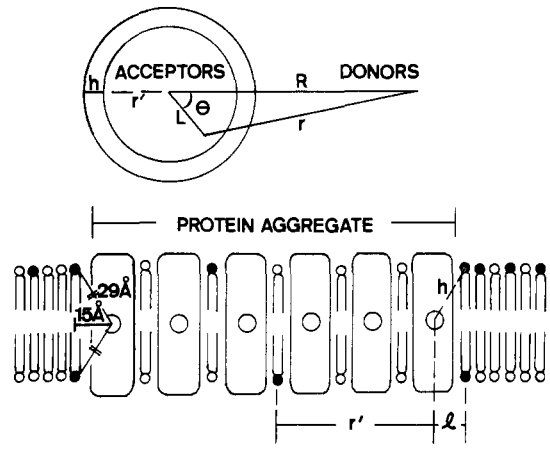

FIGURE 1: (Top) Schematic diagram of the model for resonance energy transfer from membrane aggregates. A circular patch of uniformly distributed acceptors is contained within a circle of radius, r'. This patch is separated from a plane of uniformly distributed donors by an annulus of width, h. A polar coordinate system is defined from the center of the circle. R and L are radial distrances to a donor and acceptor, respectively. The distance from a given donor to an acceptor is r, and θ is the opposite angle to r as shown in the figure. (Bottom) Schematic diagram of a membrane protein patch in a lipid bilayer. Open circles in protein represent the acceptor location. This corresponds to the retinal in bacteriorhodopsin. The distance of closest approach of a surface labeled lipid donor to the retinal is 27–31 Å. This value is used to approximate the distance h in the top diagram. The distance l is the projection of h in the plane of the membrane. The overall radius of the protein aggregate is $r' + l$. Assuming a 50-Å thickness for the bilayer and 29 Å for h, a value of 15 Å is obtained for l. The value of r' is then obtained from the energy-transfer results.

Corrected fluorescence spectra for determination of R_0 and the temperature-dependent fluorescence intensities were measured with a Spex Fluorolog 2 series spectrofluorometer equipped with a thermostated sample cell. The fluorescent intensity as a function of temperature was obtained on a Perkin-Elmer MPF-3L fluorescence spectrophotometer equipped with a Haake temperature programmer, PG11, and a Haake temperature bath, FK2. Temperatures were varied at either 12 or 18 °C/h. The temperature was recorded simultaneously with the fluorescent intensity on a strip chart recorder using an Fe–constantan thermocouple to monitor the temperature inside the sample cuvette.

Absorbances were measured on a Varian Cary 219 spectrophotometer. All samples were balanced against vesicle blanks to eliminate light scattering artifacts. Circular dichroism spectra were measured on a Jasco J 500 C spectropolarimeter.

Theory of Resonance Energy Transfer to a Circular Patch of Acceptors. A series of approximants are derived for the case of resonance energy transfer from multiple donors on a two-dimensional surface to multiple acceptors in a circular patch. A general method for deriving continued fraction approximants was presented previously (Dewey & Hammes, 1980). This method is applied to the situation illustrated in Figure 1. For the situation of multiple donors and multiple acceptors the ratio of the donor quantum yield in the presence of acceptor, Q_{DA}, to the donor quantum yield in the absence of acceptor, Q_D, is given by

$$\frac{Q_{DA}}{Q_D} = \frac{1}{N_D}\sum_j \left[1 + \sum_i \left(\frac{R_0}{R_{ij}} \right)^6 \right]^{-1} \qquad (1)$$

where the summations run over all acceptors, i, and all donors, j, and R_{ij} is the distance between the ith acceptor and the jth donor. R_0 is the characteristic Förster distance, and N_D is the

number of donors. Equation 1 can be expanded in a power series, giving

$$\frac{Q_{DA}}{Q_D} = 1 - \frac{1}{N_D}\sum_j\sum_i\left(\frac{R_0}{R_{ij}}\right)^6 + \frac{1}{N_D}\sum_j\left[\sum_i\left(\frac{R_0}{R_{ij}}\right)^6\right]^2 - \ldots$$
$$= 1 - \mu_1 + \mu_2 - \ldots \quad (2)$$

Assuming a uniform population of donors and acceptors, the nth moment of the expansion is given by

$$\mu(n) = \frac{1}{S_D}\int_{S_D}\left[\frac{N_A}{S_A}\int_{S_A}\left(\frac{R_0}{r}\right)^6 dS_A\right]^n dS_D \quad (3)$$

where S_D and S_A are the surface area of the donor region and acceptor patch, respectively, and N_A is the number of acceptors in a patch. Employing circular coordinates from the center of the patch as in Figure 1 gives $r^2 = R^2 + L^2 - 2RL\cos\theta$. Therefore

$$\mu(n) = \frac{{N_A}^n}{S_D{S_A}^n}\int_{r'+h}^{\infty} 2\pi R\, dR\left[\int_0^{r'}\int_0^{2\pi} {R_0}^6/[(R^2 + L^2 - 2RL\cos\theta)^3]\, d\theta L\, dL\right]^n \quad (4)$$

The distance, h, represents the minimal separation between an acceptor in its domain of radius r' from a donor outside of that domain. The first two moments are given by

$$\mu_1 = \frac{\pi^2 N_A {R_0}^6}{2S_D S_A h^3}\left[\frac{(r'+h)^2(r\hat{})^2}{(2r'+h)^3}\right] \quad (5)$$

$$\mu_2 = \frac{\pi^3 {N_A}^2 {R_0}^{12}(r\hat{})^4}{4S_D {S_A}^2 h^7(2r'+h)^7}\left[\frac{9}{7}(r\hat{})^4 + 4(r\hat{})^3 h + \frac{26}{5}(r\hat{})^2h^2 + \frac{16}{5}(r\hat{})h^3 + \frac{4}{5}h^4\right]$$

Two additional effects must be considered before these moments can be used to calculate approximants. First, in our experiments the fluorescent lipids are added to the bulk lipid before vesicles are prepared. Therefore, the label will be on both sides of the membrane, and energy transfer will occur from both surfaces. Our results for bacteriorhodopsin monomers are most consistent with the location of the retinal acceptor midway between the bilayer surfaces. Therefore, it is assumed that energy transfer will be identical from the two surfaces. The moments are multiplied by a factor of 2 to account for this. This can be seen by separating the summation over donors in eq 1 into two separate summations, one over each surface. The next effect to consider is due to the existence of multiple acceptor patches on the donor surface. This effect is not as straightforward. Both moments are multiplied by N_P, the number of patches. The justification for this is presented in the Appendix. This multiplicative factor is valid when the distance between patches is large and the effects of the excluded volume of a second patch on the energy transfer to a first patch is small. These factors are then introduced into the first two moments by using the following definitions.

$$\sigma_A = \frac{N_P N_A}{S_D} = \frac{N_{TOT}}{S_D} \quad (6)$$

$$\sigma_P = \frac{N_A}{S_A} =$$

(S.A. per protein + S.A. bound lipids per protein)$^{-1}$

N_{TOT} is the total number of acceptors, σ_A is the number of bacteriorhodopsin molecules per donor area, and σ_P is the surface density of bacteriorhodopsin in a patch. σ_P is calculated by assuming a surface area for the protein of 875 Å^2 (Henderson & Unwin, 1975) and 10 tightly bound lipids per protein (Heyn et al., 1981a) at 60 Å^2 per lipid. σ_A is a slightly different definition from the normal definition of surface density, $\sigma = N_{TOT}/(S_A + S_D)$. σ_A is approximately σ at low surface densities or when N_P is large (see eq 7):

$$\sigma_A = \left(\sigma^{-1} - \frac{\sigma_P^{-1}}{N_P}\right)^{-1} \quad (7)$$

The first two moments now become

$$\mu_1 = \frac{\pi^2 \sigma_A {R_0}^6 (r'+h)^2 (r\hat{})^2}{S_A h^3 (2r'+h)^3} \quad (8)$$

$$\mu_2 = \frac{\pi^3 \sigma_A \sigma_P {R_0}^{12}(r\hat{})^4}{2S_A h^7(2r'+h)^7}\left[\frac{9}{7}(r\hat{})^4 + 4(r\hat{})^3 h + \frac{26}{5}(r\hat{})^2h^2 + \frac{16}{5}(r\hat{})h^3 + \frac{4}{5}h^4\right]$$

The surface area of the patch is calculated by using $S_A = \pi(r' + 15\ \text{Å})^2$ (see Figure 1). By use of these moments, continued fraction approximants can be constructed as described previously (Dewey & Hammes, 1980). The first two approximants to Q_{DA}/Q_D are

$$A_1 = (1 + \mu_1)^{-1} \qquad A_2 = 1 - \frac{{\mu_1}^2}{\mu_1 + \mu_2} \quad (9)$$

These approximants have the convenient property of providing upper and lower bounds. The best estimate is the average of the two approximants. Thus, $Q_{DA}/Q_D \approx {}^1/_2(A_1 + A_2)$ is used as an estimate.

The error of this estimate, E, is given by $E = {}^1/_2|A_2 - A_1|$. The approximants can then be used to calculate the patch radius, r'. To do this requires that the other parameters, σ_A, R_0, σ_P, and h, are also known. R_0 and σ_A are experimentally determined, σ_P is estimated from electron diffraction data (Henderson & Unwin, 1975), and h is estimated from the distance of closest approach of a lipid to the retinal when the bacteriorhodopsin is in a monomeric state (see Figure 1).

Results

The temperature dependence of the C_{18}DiI fluorescent probe is shown in Figure 2 for DMPC vesicles with and without bacteriorhodopsin. The decrease in fluorescence intensity when bacteriorhodopsin is incorporated into the vesicles is attributed to fluorescence energy transfer to the retinal of the bacteriorhodopsin. C_{18}DiI is used at a high enough concentration so any effect due to binding of a fraction of the dye population to the protein is negligible. The energy-transfer efficiency shown in Figure 2 shows two different effects due to temperature. At low temperature the efficiency is low due to the existence of bacteriorhodopsin aggregates. In the aggregated state the protein molecules in the interior of the aggregate or patch are far from the donor lipids and cannot be effective acceptors for energy transfer. As the temperature is increased to within several degrees of the lipid phase transitions, the aggregates melt out into monomers. This effect has been observed previously (Heyn et al., 1981a,b). Circular dichroism measurements on our reconstituted system give a similar temperature dependence to these previous results. Circular dichroism melting curves are presented in the supplementary material for both DMPC and DPPC (see paragraph at end of paper regarding supplementary material). The disruption of the aggregates results in an increase in energy transfer due to the increased exposure of protein. This increase in efficiency

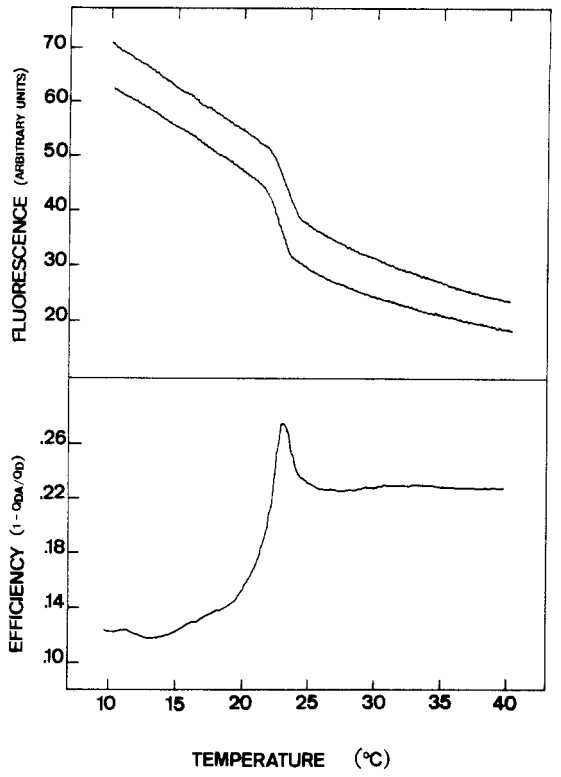

FIGURE 2: (Top) Fluorescence of C_{18}DiI in phospholipid vesicles in the presence of BR (lower fluorescent intensity) and bleached BR (greater fluorescent intensity), plotted as a function of temperature. Surface density of BR in vesicles is 4.7×10^{-5} Å^{-2}. Excitation wavelength is 540 nm; emission wavelength is 568 nm. (Bottom) Data above were used to determine efficiency of energy transfer of C_{18}DiI fluorescence, $1 - Q_{DA}/Q_D$, as a function of temperature.

is followed by a sharp decrease that occurs at the lipid phase transition. This decrease can be entirely attributed to the change in quantum yield of the fluorescent dye as it passes through the lipid phase transition. This decrease in quantum yield is shown in both of the fluorescent intensities of Figure 2. The quantum yield change results in a decreased characteristic Förster distance, R_0. The drop in energy-transfer efficiency above the lipid phase transition can be totally attributed to this change in R_0. To demonstrate this, the distance of closest approach of the lipid donor to the retinal acceptor has been measured both above and below the phospholipid phase transition. This distance is determined by measuring Q_{DA}/Q_D at various surface densities of acceptors. The distance of closest approach was then determined for each surface density by using eq 17 from Wolber and Hudson's treatment of two-dimensional energy transfer (Wolber & Hudson, 1979). A search routine was employed to find the distance of closest approach that gives the closest fit to the experimental Q_{DA}/Q_D. To determine this distance, one must know Q_{DA}/Q_D, the surface density (σ), and R_0. R_0 is defined as

$$R_0 = (JK^2Q_Dn^{-4})^{1/6}(9.7 \times 10^3 \text{ Å})$$

where n is the refractive index of the media, K^2 is an orientation factor characterizing the relative orientation of the transition dipoles of the donor and acceptor, and J is the overlap integral and is determined from the donor fluorescence and acceptor absorption spectra (Cantley & Hammes, 1975). The value of the refractive index was taken to be that of water, 1.33. K^2 was assumed to be $^2/_3$, which corresponds to the case of rapid relative motion. Results obtained with two different donor molecules were consistent, which indicates that this assumption is valid. The donor quantum yield was determined for each dye at various temperatures in both DMPC and DPPC vesicles. These values are listed in Table I. Quinine sulfate in 0.1 N sulfuric acid was used as a standard, and the quantum yield was determined by using the method of Chen (Chen, 1967). The calculated R_0 values are also listed for the various conditions in Table I. The experimental dependence of Q_{DA}/Q_D on σ is shown in Figures 3 and 4 for a variety of temperatures. Additional curves are given in the supplementary material. Values of the distance of closest approach, h, averaged over all data points, are given in Table II for all conditions observed. The solid lines in Figures 3 and 4 represent curves calculated from these average values. These results show that h is independent of temperature and is the same above and below the lipid phase transition for DMPC vesicles. Changes in the observed Q_{DA}/Q_D values are due to changes in R_0 caused by Q_D decreasing with increased temperature. Thus, the observed Q_{DA} changes can be attributed to intrinsic changes in the fluorescence of the fluorophore rather than by any changes in the distance of closest approach of donor to acceptor.

Q_{DA}/Q_D at various surface densities was also measured for bacteriorhodopsin aggregates. These results are also shown in Figures 3 and 4. These curves lie above the monomer curves because of the lower efficiency of the energy transfer. Each data point was used to calculate an aggregate or patch radius. The value of h, the distance of closest approach from the monomer data, was used as an estimate of the annulus width separating donors from acceptors (see Figure 1) in the patch. The overall patch radius is $r' + l$ where l is the projection of

Table I: Energy-Transfer Parameters

donor in lipid	temp (°C)	Q_D	R_0 (Å)[a]
C_{18}DiI in DMPC	10	0.36	55.8
	23.5	0.24	52.0
	25	0.23	51.6
	40	0.16	48.9
C_{18}DiI in DPPC	10	0.28	52.4
	20	0.22	50.4
	25	0.22	50.2
	38	0.12	45.4
OR in DMPC	10	0.49	56.2
	19	0.43	54.9
	25	0.40	54.1
	40	0.31	52.0
OR in DPPC	10	0.33	52.9
	20	0.36	53.5
	25	0.39	54.3
	38	0.37	53.8

[a] J (overlap integral) values are relatively independent of temperature. At 25 °C in DMPC (DPPC), $J = 3.97 \times 10^{-13}$ (4.02×10^{-13}) for C_{18}DiI and $J = 3.48 \times 10^{-13}$ (3.55×10^{-13}) for OR.

Table II: Summary of Results

temp (°C)	donor	lipid	protein state[a]	h (Å)	$r' + l$ (Å)
30	C_{18}DiI	DMPC	monomer	36 ± 3	
23.5	C_{18}DiI	DMPC	monomer	29 ± 7	
10	C_{18}DiI	DMPC	aggregate	29[b]	47 ± 9[c]
40	OR (C_{18})	DMPC	monomer	31 ± 2	
25	OR (C_{18})	DMPC	monomer	27 ± 6	
19	OR (C_{18})	DMPC	monomer	25 ± 5	
10	OR (C_{18})	DMPC	aggregate	29[b]	42 ± 5[c]
38	OR (C_{18})	DPPC	monomer	29 ± 4	
20	OR (C_{18})	DPPC	aggregate	29[b]	80 ± 8[c]
10	OR (C_{18})	DPPC	aggregate	29[b]	183 ± 48[c]
38	C_{18}DiI	DPPC	monomer	29 ± 1	
20	C_{18}DiI	DPPC	aggregate	29[b]	90 ± 36[c]
10	C_{18}DiI	DPPC	aggregate	29[b]	171 ± 96[c]

[a] Determined by CD measurements. [b] Monomer distance of closest approach used as an estimate of annulus width. [c] Average of surface densities above 8.0×10^{-5} Å^{-2}.

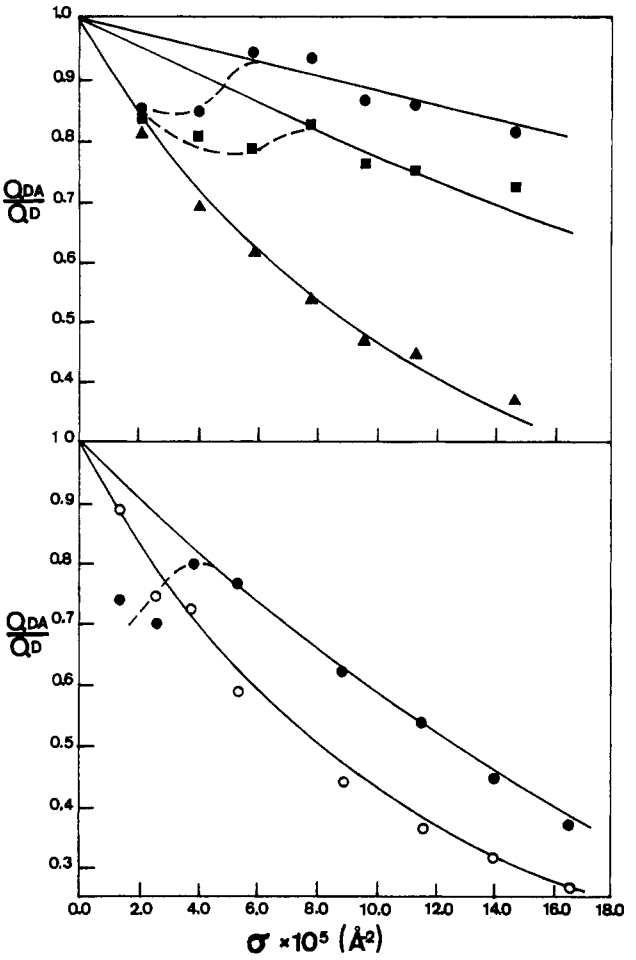

FIGURE 3: Quenching of rhodamine fluorescence by BR incorporated into phospholipid vesicles. Fluorescence in the presence of retinal acceptor divided by fluorescence in the absence of acceptor (Q_{DA}/Q_D) is plotted vs. surface density of acceptor (σ). (Top) Rhodamine incorporated into DPPC vesicles: 10 (●), 20 (■), and 38 °C (▲). (Bottom) Rhodamine incorporated into DMPC vesicles: 10 (●) and 19 °C (○). The solid curves for quenching by BR monomers (38 °C for DPPC and 19 °C for DMPC) are obtained by using the theory of Wolber and Hudson. The solid curves for quenching by BR aggregates (10 °C for DMPC and 10 and 20 °C for DPPC) are obtained from the approximate theory presented in the text. Calculated curves are for patches of a constant radius. Patch radii are given in Table II. At low temperature and low surface density of acceptor, quenching deviates from these curves (deviation shown by dashed line). This is possibly due to dissociation of the aggregates. Data points are obtained by using an excitation wavelength of 530 nm and an emission wavelength of 580 nm.

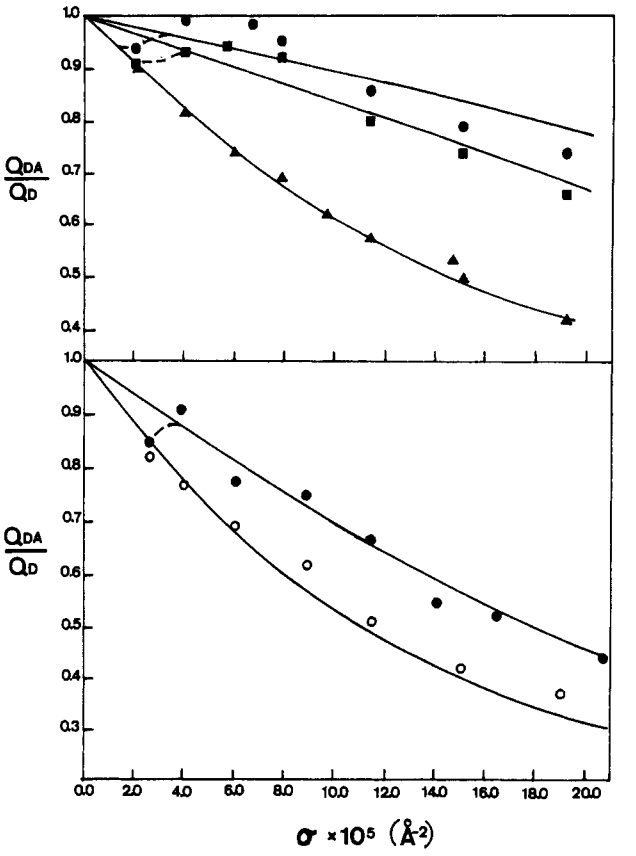

FIGURE 4: Quenching of C_{18}DiI fluorescence by BR incorporated into phospholipid vesicles. Fluorescence in the presence of the retinal acceptor divided by fluorescence in the absence of acceptor (Q_{DA}/Q_D) is plotted vs. surface density of acceptor (σ). (Top) C_{18}DiI incorporated into DPPC vesicles: 10 (●), 20 (■), and 38 °C (▲). (Bottom) C_{18}DiI incorporated into DMPC vesicles: 10 (●) and 23 °C (○). Theoretical lines are obtained as in Figure 3. BR monomers are present at 38 (DPPC) and 23 °C (DMPC). Data points are obtained by using an excitation wavelength of 540 nm and an emission wavelength of 568 nm.

h in the plane of the membrane. A value of 15 Å was taken for l (Figure 1). With these assumptions approximants from eq 9 can be used to calculate r'. At high surface densities the value of $r' + l$ was constant. These average values are given in Table II. The solid lines in Figures 3 and 4 are the curves calculated from the average values. The dashed lines indicate the deviations from the calculated curves which are observed at low surface densities. This presumably is due to aggregates dissociating at low densities.

Discussion

Protein–protein interactions in biological membranes may play a significant role in a variety of biochemical processes. Such interactions are extremely important in antibody–receptor clustering and are thought to have a direct impact on photosynthetic processes in the chloroplast thylakoid membrane (Anderson, 1981). Bacteriorhodopsin aggregates affect the rate of light and dark adaptation of the retinal chromophore (Casadio & Stoeckinius, 1980). The activity of the calcium ATPase is also affected by its state of aggregation (Ikemoto, 1983). Little is known about the nature of membrane protein aggregation and how it affects biological activity. This is in part due to a lack of techniques for investigating the structure of protein aggregates in membrane suspensions. In the present work, it is shown that resonance energy transfer can be used to determine the size of protein aggregates. With this technique the quenching due to resonance energy transfer from a fluorescent lipid label to an acceptor on the protein is observed. This quenching is quantitatively analyzed by an approximate theory presented in this paper.

A series of approximate expressions are derived for resonance energy transfer from a uniform distribution of donors in an infinite plane to a uniform distribution of acceptors in a circular patch. The patches are assumed to be identical and to exclude donors. They are also considered to be far apart from each other. For large unilamellar vesicles such as those used in the present study (Racker et al., 1979) the effects of the radius of curvature are small (Fung & Stryer, 1978). Therefore, the assumption of an infinite plane should be valid. The exclusion of the donor from an acceptor patch is a potentially more serious assumption. Our highest lipid:BR ratio is approximately 200, and it is thought that 10 lipids are tightly bound per BR (Heyn et al., 1981a). Therefore, 5% of the total lipids are in the patch at our highest protein concentration. Since the ratio of total lipid to fluorescent lipid is 200:1, it is unlikely that a large fraction of fluorescent label is located

in a patch. The observed Q_{DA}/Q_D values at this surface density of BR range from approximately 0.4 to 0.85 for a variety of conditions. In the most extreme case all the lipids in the patch are fluorescent, and the fluorescent donors in the patch are totally quenched ($Q_{DA}/Q_D = 0$). This would decrease the observed Q_{DA}/Q_D by approximately 2–4%. Thus, this second assumption will not seriously alter our results. The issue of distance between patches is addressed in detail in the Appendix. The assumption of uniform patch size is clearly the weakest one. In practice the patch radius must be considered to be a patch number weighted average over all patch radii. Because of potential heterogeneity in patch sizes one must be careful in interpreting the patch radius, and it must be realized that this value will represent a complicated average of the patch size distribution.

To establish this technique and theoretical analysis, protein aggregation in a well-defined reconstituted system was investigated. Bacteriorhodopsin reconstituted into DMPC or DPPC vesicles offers such a system. It has been established by a variety of techniques (Heyn et al., 1981a,b) that bacteriorhodopsin will aggregate at temperatures well below the lipid phase transition. The state of aggregation can be easily varied by changing the temperature. An additional advantage is that the retinal of bacteriorhodopsin provides a convenient acceptor for energy transfer. Neutron diffraction studies indicate that this chromophore is located approximately in the middle of the lipid bilayer (King & Schoenborn, 1982). Most recent work favors the location of the retinal at lysine-216 (cf. Stoeckenius & Bogomolni, 1982; Ovchinnikov, 1982) which from molecular models would put the chromophore halfway through the bilayer. Recent energy-transfer results show the distance of closest approach from the reduced retinal to a cobalt–EDTA complex to be 8–9 Å (Kouyama et al., 1983). For our monomer results to be consistent with this shorter depth the radius of bacteriorhodopsin must be approximately 28 Å. This is an unrealistically large radius. Locating the retinal at the midpoint of the bilayer is more consistent with the distance of closest approach of 29 Å obtained from our energy-transfer results for monomeric bacteriorhodopsin. This represents the closest distance between a lipid with a donor at the membrane surface and the retinal (distance h in Figure 1). Assuming a 50-Å bilayer and a distance of closest approach of 29 Å from either side of the membrane, 15 Å is calculated for the distance from the retinal to the closest periphery of the protein. This agrees with the result for energy transfer from diphenylhexatriene to retinal (Rehorek et al., 1983). This membrane-soluble fluorescent probe has a distance of closest approach of 18 ± 5 Å which would correspond to the distance l in Figure 1. The distance of closest approach obtained in this work for two different donors at temperatures above and below the lipid phase transition range from 25 to 31 Å for OR and from 29 to 36 Å for C_{18}DiI. The small variation in these results suggests that the assumption of rapid relative rotation of the donor and acceptor is probably valid. This assumption requires that the value for K^2 be $^2/_3$. This value is used throughout in calculating R_0. Slightly longer distances obtained with C_{18}DiI are presumably due to the fact that C_{18}DiI, containing two fatty acids, is a bulkier probe. It is important to establish the distance of closest approach for monomeric bacteriorhodopsin before proceeding with an analysis of aggregated protein. This distance provides a convenient estimate for the width of the annulus separating the patch of acceptors from the donors in the membrane. The overall patch radius, $r' + l$, that is determined from the data may be a sensitive function of the value chosen for h. This

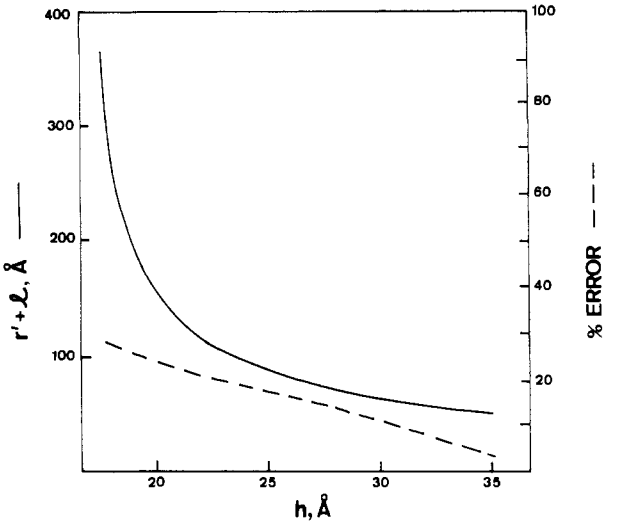

FIGURE 5: Plot of overall patch radius, $r' + l$ (solid line), as a function of the annulus width, h. Assuming a value of h and using eq 9 of the text, $r' + l$ was calculated for rhodamine in DPPC vesicles at 20 °C. The bacteriorhodopsin surface density was 13.3×10^{-5} Å^{-2}, and an assumed value of Q_{DA}/Q_D was 0.76. The value for l is 15 Å, and R_0 is 53.5 Å. The broken line (right hand scale) indicates the error of the estimates.

is illustrated in Figure 5 where the patch radius has been calculated from an experimental data point assuming different values for h. As can be seen from the plot, the radius can increase dramatically at small values of h. This plot indicates that at a given energy-transfer efficiency a decrease in h is compensated by an increase in the patch radius. Thus, it is important to have a reasonable estimate of the distance, h.

In general the energy-transfer efficiency is a complicated function of R_0, surface density, patch size, and annulus width. However, the results given in Table II can give some indication of the practical limits of the technique. In the conditions of these experiments patch radii ranging from 30 to 300 Å would be measured easily and accurately. The limits of the radius determination will vary with R_0 but should be of the same order of magnitude as in these experiments. Using the first two moments to estimate Q_{DA}/Q_D usually gives errors for the approximation of around 10%. This is reasonably accurate for the current level of sophistication of the experiment. As is seen in Figure 5 the error of the approximation can become much larger as h decreases. In such cases it may be beneficial to include the third moment in the calculation. However, the third approximant may be difficult to evaluate analytically due to the effects of multiple patches in a membrane (see Appendix). One advantage of this theoretical analysis is that it provides a direct measure of the accuracy of the approximations used.

The results on the size variation of bacteriorhodopsin aggregates reveal some interesting aspects of the aggregation phenomenon. First, there appears to be a range of surface densities in which a constant average patch size is formed. At low surface densities the patches may break up into smaller units. The experimental curves approach those of bacteriorhodopsin monomers at these lower densities. This is seen more clearly in the case of DPPC vesicles and is evident to a lesser extent in DMPC vesicles (Figures 3 and 4). This effect is currently under investigation. While our results cannot exclude the possibility that monomers are in equilibrium with aggregates at high surface density, such a model would be inconsistent with the circular dichroism melting curve and the rotational diffusion constant for bacteriorhodopsin (Heyn et al., 1981b). These results indicate that bacteriorhodopsin is im-

mobilized in a semicrystalline array at the temperature and surface densities of our experiments. Unfortunately there is little previous experimental evidence that specifically relates to patch size. Rotational diffusion constants of bacteriorhodopsin patches in DMPC vesicles were measured at two different lipid to protein ratios (111 and 168) (Heyn et al., 1981b). These constants are very similar over most temperatures and are identical at 10 °C where our experiment was done. Since the rotational diffusion constant is proportional to the inverse of the patch radius squared, this result suggests a constant patch size. Electron microscopy has been done on bacteriorhodopsin reconstituted into DMPC and DPPC vesicles at the extremely high lipid to protein ratio of 4:1 (Cherry et al., 1978). These results show irregular structures, with DPPC tending to form larger patch networks. Our lipid to protein ratios are 200:1 or more and cannot be compared with the electron microscopy work. However, our results do show that DPPC patch areas are fourfold larger than DMPC patch areas. Thus, specific protein–lipid interactions would appear to have a large effect on the aggregation process. The average patch size is also dependent on temperature. For DPPC vesicles the overall patch radius increases by about a factor of 2 with a drop of temperature by 10 °C. This indicates a noticeable favorable enthalpy contribution for aggregate formation. These results demonstrate the utility of this technique for investigating membrane protein aggregation phenomena. Our future applications will include more detailed studies of bacteriorhodopsin aggregates and new studies of the association of the calcium ATPase from sarcoplasmic reticulum.

Appendix

Two-Dimensional Resonance Energy Transfer to Multiple Circular Patches. The theoretical development of this paper deals with resonance energy transfer from a planar array of donors to a single circular patch of acceptors. Multiple patches of acceptors will have two main effects on this energy transfer. First, in calculating energy transfer to a single patch the surface area excluded by the other patches has not been accounted for in the paper. At the surface densities of bacteriorhodopsin used in this work (less than 10% total surface area) this will not be a large effect. If the patches are uniformly distributed, they should be far enough apart that the donor surface excluded by neighboring patches will have a negligible effect on energy transfer to any given patch. The second effect is due to certain integrals that arise in the averaging of the moment expansion (Figure 6). These integrals represent simultaneous averages over two or more patches. These two center integrals have been assumed to make a negligible contribution to the overall energy transfer process. To justify this, energy transfer to multiple patches must be introduced into the formalism of this paper. By use of eq 1, the separate patches are included by separating the summation over all acceptors into summations over acceptors in individual patches. Thus, a double summation is introduced:

$$\frac{Q_{DA}}{Q_D} = \frac{1}{N_D}\sum_j \left[1 + \sum_P \sum_i \left(\frac{R_0}{R_{Pij}} \right)^6 \right]^{-1}$$

where the summation over all patches, P, is included. The series expansion of this gives

$$\frac{Q_{DA}}{Q_D} = \frac{1}{N_D}\sum_j \left[1 - \sum_P \sum_i \left(\frac{R_0}{R_{Pij}} \right)^6 + \left(\sum_P \sum_i \left(\frac{R_0}{R_{Pij}} \right)^6 \right)^2 - \dots \right]$$

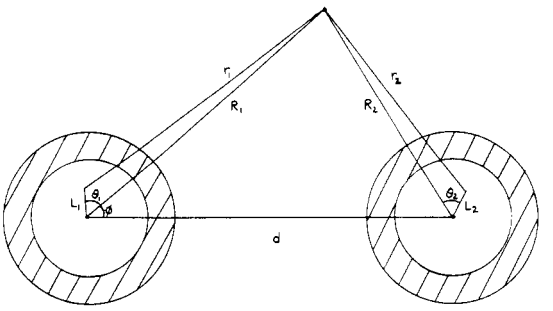

FIGURE 6: Schematic diagram of resonance energy transfer coordinates for two circular patches of acceptors. L and θ are polar coordinates centered at each patch. The distance between a donor and an acceptor is r, and d is the distance between the center of the two patches. The angle ϕ is defined as indicated on the diagram. Hatched areas represent regions separating donors from acceptors.

If identical patches are assumed, the summation, i, over acceptors within a patch will be identical and the first moment will contain a multiplicative term, N_p, for the number of patches. The second moment has two different types of terms:

$$\mu_2 = \frac{N_P}{N_D}\sum_j \left[\sum_i \left(\frac{R_0}{R_{Pij}} \right) \right]^2 + \frac{1}{N_D}\sum_j \sum_P \sum_{P'} \sum_i \left(\frac{R_0}{R_{Pij}} \right)^6 \left(\frac{R_0}{R_{P'ij}} \right)^6 \qquad P \neq P'$$

The first term contains squared contributions from the same patch while the second term contains contributions from two different patches. There are N_p $(N_p - 1)$ terms in this second term. Since all the patches are separated by different distances, this second term is not further simplified. In this paper, only the first term in μ_2 was used. Thus, in this case, the effect of multiple patches is to again multiply the single patch moment by N_p. It is assumed that the two center contributions in the second term are small. This is because the patches will be far apart and donors that contribute strongly to the multiplicative term from one patch will have negligible contributions from the multiplicative term from a second patch. The two center integral will be

$$\int_{S_D} dS_D \left[\int_{S_{A_1}} \left(\frac{R_0}{r_1} \right)^6 dS_{A_1} \right] \left[\int_{S_{A_2}} \left(\frac{R_0}{r_2} \right)^6 dS_{A_2} \right] = \int_{S_D} d\theta R_1 \, dR_1 \left[\frac{(r')^4 + 2R_1^2(r')^2}{2[R_1^2 - (r')^2]^4} \right] \left[\frac{(r')^4 + 2R_2^2(r')^2}{2[R_2^2 - (r')^2]^4} \right]$$

Using Figures 1 and 6 and the relationship

$$R_2^2 = R_1^2 + d^2 - 2R_1 d \cos\phi$$

where d and ϕ are defined in Figure 6 give

$$\int d\phi R_1 \, dR_1 [[(r')^4 + 2R_1^2(r')^2]/[2[R_1^2 - (r')^2]^4]] \times [[(r')^4 + 2(r')^2(R_1^2 + d^2 - 2R_1 d \cos\phi)]/[2[R_1^2 + d^2 - 2R_1 d \cos\phi - (r')^2]^4]]$$

The largest term in the integrand will contain a multiplicative factor of d^{-6}. The distance, d, between patches will vary for each pair. The closest average distance can be roughly estimated. Assuming a vesicle radius of 1000 Å and a protein surface density of 10^{-4} Å^{-2}, there are approximately 1000 molecules per vesicle. Assuming 10 molecules per patch gives a distance of approximately 600 Å between patches. The factor of d^{-6} will make the relative contributions of these two center integrals small. They have, therefore, not been included in the second moment. The higher moments will contain even higher order integrals, some of which may be significant.

However, the first two approximants give reasonable error estimates, and higher order moments are not considered.

Supplementary Material Available

One plot of Q_{DA}/Q_D vs. BR surface density for DMPC vesicles with rhodamine B chloride at 25 and 40 °C and C_{18}DiI at 30 °C and one plot of ellipticity (θ) at 590 nm vs. temperature (°C) for BR reconstituted into DMPC vesicles (open circles) or DPPC vesicles (closed squares) (2 pages). Ordering information is given on any current masthead page.

Registry No. DMPC, 13699-48-4; DPPC, 2644-64-6; C_{18}DiI, 41085-99-8; OR, 65603-19-2.

References

Anderson, J. M. (1981) *FEBS Lett. 124*, 1-10.

Baird, B. A., Pick, U., & Hammes, G. G. (1979) *J. Biol. Chem. 254*, 3818-3825.

Becher, B. M., & Cassim, J. Y. (1975) *Prep. Biochem. 5*, 161-178.

Cantley, L. C., Jr., & Hammes, G. G. (1975) *Biochemistry 14*, 2976-2981.

Casadio, R., & Stoeckenius, W. (1980) *Biochemistry 19*, 3374-3381.

Chen, R. (1967) *Anal. Biochem. 19*, 374-387.

Cherry, R. J., Mueller, U., Henderson, R., & Heyn, M. P. (1978) *J. Mol. Biol. 121*, 283-298.

Dewey, T. G., & Hammes, G. G. (1980) *Biophys. J. 32*, 1023-1036.

Ebrey, T. G., Becher, B., Mao, M., Kilbride, P., & Honig, B. (1977) *J. Mol. Biol. 112*, 377-397.

Fleming, P. J., Koppel, D. E., & Strittmatter, P. (1979) *Biochemistry 18*, 5458-5464.

Fung, B. K.-K., & Stryer, L. (1978) *Biochemistry 17*, 5241-5248.

Hammes, G. G. (1981) *Protein-Protein Interaction*, pp 257-287, Wiley, New York.

Henderson, R., & Unwin, P. N. T. (1975) *Nature (London) 257*, 28-32.

Heyn, M. P., Blume, A., Rehorek, M., & Dencher, N. A. (1981a) *Biochemistry 20*, 7109-7115.

Heyn, M. P., Cherry, R. J., & Dencher, N. A. (1981b) *Biochemistry 20*, 840-849.

Ikemoto, N. (1982) *Annu. Rev. Physiol. 44*, 297-318.

King, G. I., & Schoenborn, B. P. (1982) *Methods Enzymol 88*, 241-248.

Kouyama, T., Kinosita, K., & Ikegami, A. (1983) *J. Mol. Biol. 165*, 91-107.

Lanyi, J. K., & MacDonald, R. E. (1979) *Methods Enzymol. 56*, 398-407.

Ovchinnikov, Y. A. (1982) *FEBS Lett. 148*, 179-191.

Racker, E., Violand, B., O'Neal, S., Alfonzo, M., & Telford, J. (1979) *Arch. Biochem. Biophys. 198*, 470-477.

Rehorek, M., Dencher, N. A., & Heyn, M. P. (1983) *Biophys. J. 43*, 39-45.

Snyder, B., & Freire, E. (1982) *Biophys. J. 40*, 137-148.

Stoeckenius, W., & Bogomolni, R. A. (1982) *Annu. Rev. Biochem. 52*, 587-616.

Stryer, L. (1978) *Annu. Rev. Biochem. 47*, 819-846.

Wolber, P. K., & Hudson, B. S. (1979) *Biophys. J. 28*, 197-210.

Cardiolipin Conformation and Dynamics in Bilayer Membranes As Seen by Deuterium Magnetic Resonance†

Peter R. Allegrini, Gerd Pluschke, and Joachim Seelig*

ABSTRACT: Deuterium nuclear magnetic resonance was used to investigate the structure and dynamics of the cardiolipin polar region in pure cardiolipin bilayers and in mixed cardiolipin–lecithin systems. The *Escherichia coli* mutant B 131GP defective in both the biosynthesis and degradation of glycerol was used for biosynthetic labeling of cardiolipin. Deuterated glycerol added to the growth medium was specifically incorporated into membrane phospholipids, and deuterated cardiolipin was purified from lipid extracts. Deuterium NMR spectra yielded characteristic quadrupole splittings that could be assigned to the corresponding backbone and head-group deuterons. Both glycerol backbones in cardiolipin were found to adopt identical conformations. As observed in other lipids, the glycerol backbones of cardiolipin are oriented perpendicular to the bilayer surface. The glycerol head group of cardiolipin was distinctly less flexible than the polar groups of other lipids as suggested by T_1 relaxation time measurements. Only small changes in the quadrupole splittings could be detected between a pure cardiolipin bilayer and a mixed cardiolipin lecithin system.

In 1906 Wassermann demonstrated the presence of specific antibodies in the sera of syphilis patients (Wassermann et al., 1906) against an antigen that later turned out to be cardiolipin (Pangborn, 1942). Cardiolipin can be found in the membranes of almost all organisms. When different human organs are compared, the largest percentage of cardiolipin is present in heart and skeletal muscle (Rouser et al., 1969; Simon & Rouser, 1969). Furthermore, it is characteristically associated with subcellular membranous particles displaying high metabolic activity, e.g., mitochondria. The cardiolipin content of a particular membrane can be influenced by a number of different biological processes such as aging (Bruce, 1974), transition from exponential to stationary growth phase [yeast (Jakovcic et al., 1971); *Escherichia coli* (Kanemasa et al., 1967)], or infection of *E. coli* [bacteriophage f1 (Chamberlain & Webster, 1976)]. The chemistry and biochemistry of cardiolipin have been reviewed recently (Ioannou & Golding, 1979).

Studies with a mutant deficient in the synthesis of cardiolipin have suggested that this lipid is a dispensable component of

† From the Department of Biophysical Chemistry, Biocenter, University of Basel, CH-4056 Basel, Switzerland (P.R.A. and J.S.), and the Max-Planck-Institut für Molekulare Genetik, D-1000 Berlin, West Germany (G.P.). *Received April 6, 1984.* This work was supported by Swiss National Science Foundation Grant 3.294.82.

0006-2960/84/0423-6452$01.50/0